Colloidal crystal photothermal dynamics

R. Kesavamoorthy,[a] S. Jagannathan, Paul A. Rundquist, and Sanford A. Asher[b]
Department of Chemistry, University of Pittsburgh, Pittsburgh, Pennsylvania 15260

(Received 29 October 1990; accepted 17 December 1990)

Localized heating of a colloidal crystal by absorption of high intensity laser radiation (>25 W/cm^2) results in compression of the hot region. The time dependent variations in the lattice spacing of the crystal due to this local heating has been studied by monitoring the transmission profile of a weak laser beam incident on the crystal at an angle close to the Bragg angle. The dynamics of the compression phenomenon and its subsequent relaxation after removing the pump laser beam are analyzed using the screened Coulomb pair potential formulation. A simple linear model is developed to explain the deformation of the crystal during both the heating and cooling processes. Using this model we estimate the time dependent temperature rise in the crystal for any given pump power. During the heating process and the early stages of cooling the change in the crystal lattice spacing lags behind the rate of temperature change, while during the later stages of cooling it follows the rate of cooling. We demonstrate the necessity for the renormalization of the surface charge of colloidal particles when using the screened Coulomb pair potential.

INTRODUCTION

Colloidal crystals of charged polymer particles are used extensively to study colloidal interactions in concentrated dispersions.[1-5] The dominant interaction in these systems is the electrostatic repulsion between the charged particles which is screened by mobile counterions in the medium.[6] The interactions between colloidal particles having a small surface charge is explained by the screened Coulomb pair potential (DLVO theory).[7,8] When the surface charge on the particles is high, the interaction potential falls off much more rapidly than would be predicted by this model. It has been suggested that it is possible to use this model for highly charged particles if the surface charge is renormalized to a smaller effective charge.[9] The effectiveness of the renormalization procedure and the conditions under which this is necessary have not been clearly established.

The interactions in colloidal crystals are generally studied by monitoring the optical properties of the crystals. By carefully varying the particle concentration and the ionic strength of the dispersion, the lattice spacing in colloidal crystals can be varied over a range of hundreds of nanometers.[10] Due to this unique ability to experimentally vary the lattice spacing, colloidal crystals can be made to diffract light in the ultraviolet, visible and infrared regions of the electromagnetic spectrum.[11-13] The diffraction phenomenon is sensitive to a number of parameters such as the lattice spacing, particle size, refractive index mismatch between the particles and the medium, defects in the crystal and the thermal vibrations of the particles.[14,15] Hence diffraction has proved to be an excellent probe of colloidal interactions in concentrated dispersions. Diffraction has been used extensively to study the effect of shear,[16] gravity,[17-19] electric field,[20] pressure,[21] and temperature[22-24] on colloidal interactions.

The evolution of a colloidal crystal (towards a new equilibrium state) under the influence of an external field like gravity has been studied previously.[25,26] Recently we reported that dyed colloidal crystals show localized compression under the influence of a temperature field created by a laser beam.[27] This phenomenon is a direct consequence of the negative temperature dependence of the screened Coulomb pair potential; the temperature increase perturbs the equilibrium lattice of the colloidal crystal which is defined completely by the temperature dependent interaction potential. For the crystals studied here the perturbation (or deformation) results in a compression of the lattice (without any change in the crystal structure). We utilize a linear response model to describe the dynamics of the colloidal crystal response to this temperature perturbation. The only temperature dependent parameter in the model is the electrostatic repulsive interaction between particles. Using our model we obtain the linear deformation and temperature rise in the heated region for various pump powers and pump durations. We demonstrate the necessity for renormalizing the charge on the particles and describe a procedure to estimate the charge renormalization required.

EXPERIMENT

A detailed account of the experimental procedure and the experimental results are provided in our previous work.[27] The colloidal crystal used in the study was prepared from 83 nm polystyrene particles that had 2370 negative charges per particle. The particles contained a nonfluorescent red dye (Oil Red O) which has a broad absorption maximum around 520 nm. Large BCC single crystals of the dyed particles having dimensions of $2.5\times2.5\times0.05$ cm were prepared according to reported procedures.[14] The particle concentration in the crystal was 8.85×10^{13} cm^{-3} and the crystal structure was established by Kossel ring analysis. The photothermal experiments were carried out using the 514.5 nm line of an argon ion laser as the pump (heating)

[a] Materials Science Division, Indira Gandhi Centre for Atomic Research, Kalpakkam 603 102, India
[b] Author to whom correspondence should be sent.

 0021-9606/91/075172-08$03.00

beam and the 488 nm line from the same laser as the probe beam. For this purpose the laser was operated in the multiwavelength mode and the required wavelengths were isolated outside the laser cavity using a diffraction grating. The pump and probe beams were overlapped on a 0.2 mm spot in the sample. The transmittance of the weak probe beam through the crystal during and after heating by the pump beam was detected with a fast photodiode and recorded on a digitizing oscilloscope. The variation in the transmitted intensity of the probe results from alterations in the Bragg angle which changes in response to changes in the lattice parameters. The crystals were oriented such that the angle of incidence of the probe beam was either slightly lower or slightly greater than the Bragg angle. Figure 1 shows the typical experimental result observed when the probe beam is incident at an angle slightly greater than the Bragg angle. For this geometry the transmitted intensity decrease derives from a decrease in the lattice spacing and a resulting increase in the Bragg angle.[27] The Bragg condition becomes more closely met and the transmittance decreases. In analogous manner, a transmitted intensity increase would accompany a lattice spacing increase.

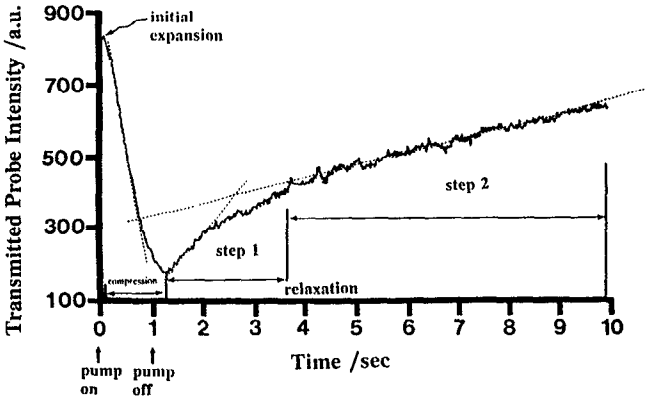

FIG. 1. A transmission curve from a photothermal study of an absorbing colloidal crystal (see text for details). The angle of incidence of the probe beam is 1.5° greater than the Bragg angle. Pump power = 50 mW and pump duration = 1 s.

THEORY

Consider a colloidal crystal illuminated by a pulsed Gaussian laser beam. The absorption of this laser beam by the colloidal crystal leads to an approximately Gaussian temperature profile in the crystal.[28] For simplicity, we approximate this temperature profile by a triangular function, as shown in Fig. 2. The maximum temperature rise ΔT in the sample is at the center of the beam and falls off linearly to room temperature (298 K) at the edge of the beam (0.1 mm from the center). The temperature of different regions in the illuminated volume lie between 298 K and $(298 + \Delta T)$ K. This gradient in temperature also gives rise to a gradient in the interparticle interaction potential. The differences in the interaction potential between adjacent regions results in a driving force that evolves the colloidal crystal towards a new equilibrium configuration. We assume a linear response of the colloidal crystal to the temperature increase. Hence, the deformation of the crystal is linear since the temperature profile is linear.

The temperature dependent screened Coulomb pair potential is given by

$$U(r,T) = \frac{Z^2 e^2}{\epsilon}\left(\frac{e^{\kappa a}}{1+\kappa a}\right)^2 \frac{e^{-\kappa r}}{r}, \tag{1}$$

where Z e, and a are the charge and the radius of the particle, r is the interparticle separation distance and κ is the inverse Debye length of the system:

$$\kappa^2 = \frac{4\pi e^2}{\epsilon k_B T}(n_p Z + n_i), \tag{2}$$

where n_p is the particle number concentration, n_i the ionic impurity concentration and k_B the Boltzmann constant. Because the surface charge is provided by a strong acid group (sulfonic acid) we assume that the extent of dissociation is not temperature dependent; the dielectric constant, ϵ is the only parameter that is directly sensitive to temperature. The temperature dependence of ϵ for water is given by[27]

$$\epsilon = \frac{A}{T^{1.5}} + \frac{B}{T} + \frac{C}{T^{0.5}} + D \tag{3}$$

for T in the range 290 K to 360 K, and $A = -439\,481.41$, $B = 72\,528.68$, $C = -314.08$, and $D = -61.45$.

The temperature dependence of the derivative of the interaction potential $\partial(U(r,T))/\partial T$ is shown in Fig. 3. $\partial(U(r,T))/\partial T$ is negative in the temperature range of interest (298 K). This indicates that the colloidal crystal will undergo compression upon heating, because the interaction potential in the heated region becomes less than that of the surrounding colder regions (298 K).

The situation is more complex, however, because the sample photothermal response depends upon the tempera-

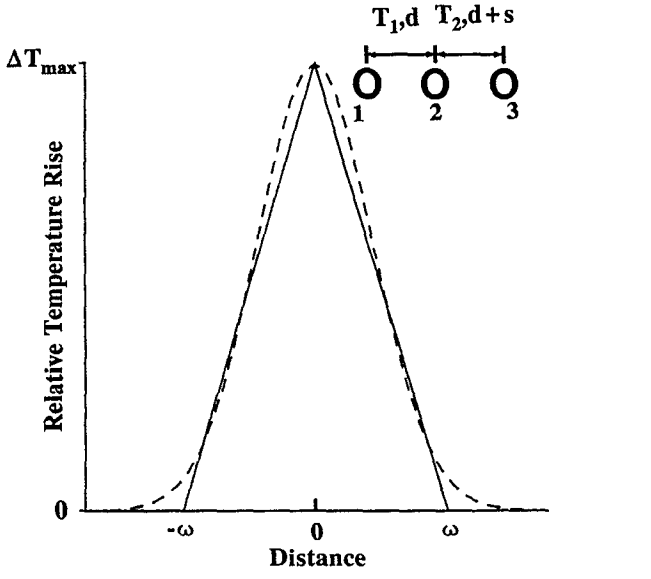

FIG. 2. The modeled triangular spatial temperature profile in the colloidal crystal induced by the pump laser beam. The inset is a schematic representation of a linear array of particles within the heated region.

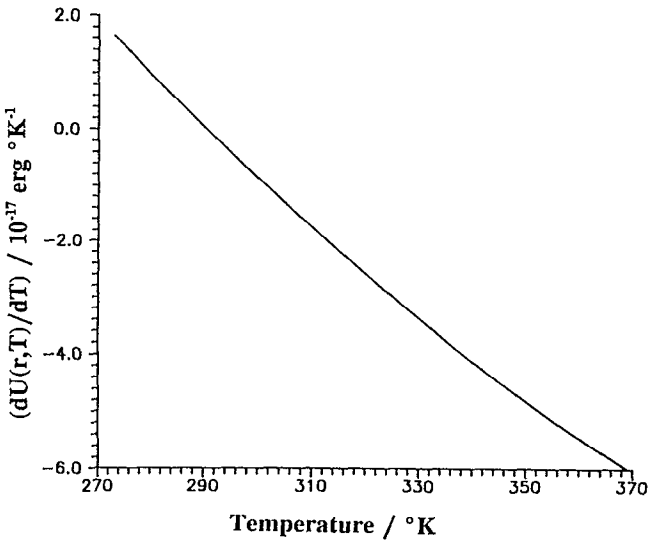

FIG. 3. Plot of the temperature derivative of the interaction potential as a function of temperature.

ture dependence of the force ($-\partial U(r,T)/\partial r$). We can calculate this force by considering the linear array of particles shown in Fig. 2. Let the repulsive interaction potential between particles 1 and 2 be given by $U(T_1,d)$ and the potential between particles 2 and 3 by $U(T_2,d+s)$, where $T_1 > T_2$, d is the distance between the particles 1 and 2 and s is the linear perturbation in d due to the increase in temperature. The net repulsive force between particles 1 and 2 is given by $-\partial [U(T_1,d)]/\partial r$ and the force between particles 2 and 3 by $-\partial [U(T_2,d+s)]/\partial r$. The net force on particle 2 is given by

$$\Delta F = -\frac{\partial}{\partial r}[U(T_1,d)] + \frac{\partial}{\partial r}[U(T_2,d+s)]. \quad (4)$$

Because the temperature difference $(T_1 - T_2)$ and the change in interparticle spacing (s) is small, $U(T_1,d)$ can be expanded in a Taylor series:

$$U(T_1,d) = U(T_2,d+s) + \frac{\partial U(T_2,d+s)}{\partial T}(T_1 - T_2) - \frac{\partial (T_2,d+s)}{\partial r} s. \quad (5)$$

Neglecting the higher order terms

$$\Delta F = -\frac{\partial}{\partial r}\left(\frac{\partial U(T_2,d+s)}{\partial T}(T_1 - T_2) - \frac{\partial U(T_2,d+s)}{\partial r} s\right). \quad (6)$$

Let $U(T_2,d+s) = U$ and $T_1 - T_2 = \delta T$. Because δT and s are constant with respect to variations in r:

$$\Delta F = \delta T\left\{\frac{\partial}{\partial T}\left[-\frac{\partial U}{\partial r}\right]\right\} + s\left[\frac{\partial^2 U}{\partial r^2}\right]. \quad (7)$$

The only temperature dependent term in Eq. (7) is the repulsive force between the particles and Eq. (7) can be rewritten as

$$\Delta F = \delta T\left[\left(\kappa + \frac{1}{d}\right)\frac{\partial U}{\partial T} + U\frac{\partial \kappa}{\partial T}\right] + sU\left[\kappa^2 + \frac{2\kappa}{d} + \frac{2}{d^2}\right]. \quad (8)$$

In our case δT, U, κ, $\partial\kappa/\partial T$ are positive and $\partial U/\partial T$ is negative. Using Eq. (8) for the force acting on particle 2 due to the spatial temperature gradient, we can consider the situation close to $t = 0$, i.e., when the pump is just turned on. At times slightly greater than $t = 0$, $s = 0$; the interparticle spacing is the same throughout the crystal. This means that ΔF is determined by the first term in Eq. (8), which is the temperature dependence of the repulsive force between particles. If this term is positive [i.e., $(\kappa + 1/d)|\partial U/\partial T| < U\partial\kappa/\partial T$] then ΔF is positive, the hot region expands and particle 2 moves towards particle 3 (s becomes negative) to balance this force. If $(\kappa + 1/d)|\partial U/\partial T| > U\,\partial\kappa/\partial T$, ΔF becomes negative and the hot region contracts and particle 2 moves towards particle 1 (making s positive) to balance this force. It is really the sign of the product $(\delta T[\partial(-\partial U/\partial r)/\partial T])$ that determines whether the heated region in the crystal expands or contracts.

When the crystal is heated continuously δT increases monotonically and s increases or decreases to balance the resultant driving force (ΔF). If the product $\delta T[\partial(-\partial U/\partial r)/\partial T]$ initially increases with temperature and then attains a maximum value and then decreases, the hot region will initially expand. Thus, s will initially be negative and attain a minimum value and then will increase in a positive direction as the crystal contracts. In such a case, the crystal strain driving force is zero when s is a minimum. Alternatively, $\delta T[\partial(-\partial U/\partial r)/\partial T]$ may go through a minimum with temperature, and thus s will go through a maximum. In such case, the driving force is zero at maximum s. It will also be zero at steady state when the particles cease to move any further due to the attainment of thermal equilibrium where the heat input is equal to the rate of heat lost to the surroundings.

During the time course of our experiments the system continues to evolve. Upon heating we observe an expansion which then changes to contraction. This indicates that s decreases initially, reaches a minimum value and then increases. This can be seen in Fig. 1, which shows the transmitted probe intensity (incident at an angle slightly greater than the Bragg angle) vs time when the crystal was heated by a 50 mW pump beam for 1 s. It starts expanding again about 100 ms after turning off the pump. $\Delta F = 0$ at the extremes of the transmittance curve.

We can calculate the value of s that makes $\Delta F = 0$ for various values of ΔT, i.e.,

$$\Delta F = 0 = \delta T\left[\left(\kappa + \frac{1}{d}\right)\frac{\partial U}{\partial T} + U\frac{\partial \kappa}{\partial T}\right] + sU\left[\kappa^2 + \frac{2\kappa}{d} + \frac{2}{d^2}\right]. \quad (9)$$

If ΔT is the difference in temperature between the center of the hot region and the edge and the radius of the beam is $\omega \approx 0.1$ mm:

$$\delta T = \frac{\Delta T}{\omega} d. \tag{10}$$

The values of $\partial U/\partial T$, κ, U, $\partial\kappa/\partial T$ depend on temperature and hence the position of particle 2. Let particle 2 be midway between the center and the edge of the hot region. Then $\partial U/\partial T$, κ, U, $\partial\kappa/\partial T$ can be calculated at $T = 298 + \Delta T/2$. Because d can be obtained from diffraction measurements, the value of s for various values of ΔT can be calculated using Eqs. (9) and (10). Figure 4 shows the calculated dependence of s/d upon ΔT. From this plot and the experimental data (the maximum values of s/d for various pump powers and pump duration) we can estimate the maximum temperature rise (ΔT_{max}) in the crystal for different pump powers and pump durations.

From Fig. 1 it may be seen that the hot region of the crystal continues to contract for about 100 ms after turning off the pump, before starting to expand towards the preheated value. This relaxation phenomenon appears to be a two step process. When the pump is turned off, heat input ceases, but the hot region possesses a temperature gradient. The time constant for the thermal equilibration of the hot region is given[28] by $\tau_T = \omega^2/4D_T \approx 18$ ms (where D_T, the thermal diffusivity of water is ca. 1.46×10^{-3} cm^2 s^{-1}). The mean temperature and the temperature gradient of the hot region decreases with this ca. 18 ms time constant; however, the value of s cannot change significantly during this short cooling time period because the collective diffusion coefficient (D_c) which determines the crystal strain relaxation rate, is much smaller. The collective diffusion coefficient of the particles can be determined from the following expression:[29,30]

$$D_c = \frac{D_0}{n_p k_B T}(B + \tfrac{4}{3}C), \tag{11}$$

where D_0 ($= k_B T/6\pi\eta a$) is the free particle diffusion coefficient, C ($= 4n_p U(\kappa d)^2/9$) is the shear modulus and B ($= 4n_p U(\kappa d + 2)^2/9$) is the bulk modulus of the crystal.[31] For our crystal $D_c = 3.5\times10^{-6}$ cm^2 s^{-1} which gives a resulting time constant (τ_p) for the response of the lattice of ca. 7.2 s. This slow particle response time results in a large driving force [because the second term in Eq. (8) becomes very large], and the region previously heated expands rapidly. This rapid expansion is the first step of the relaxation

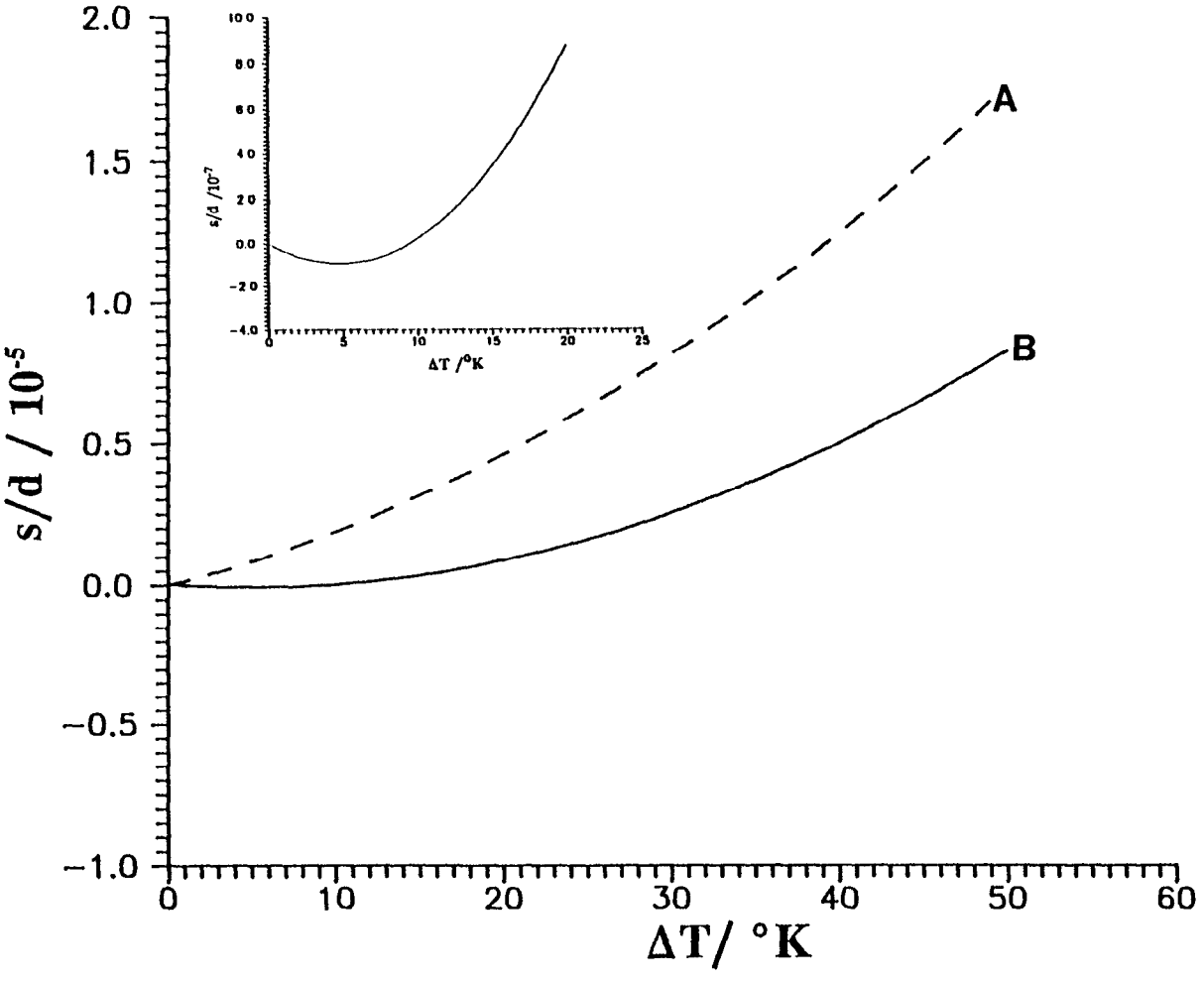

FIG. 4. Plot of the strain of the crystal as a function of the temperature rise [Eq. (9)]. Curve A was computed using the measured surface charge of 2370 and curve B utilized a renormalized surface charge of 1150. The inset shows an expanded version of plot B.

process. During this first step, s decreases rapidly causing the driving force to decrease. In the second step of the relaxation process, the driving force is sufficiently small that s follows the cooling. Hence, the rate of cooling can be estimated from the slope of the second step of the relaxation curve (vide infra).

RESULTS AND DISCUSSION

Figure 4 shows the values of s/d which make the driving force (ΔF) zero for various values of ΔT. Curve A was obtained for a colloidal crystal having a particle concentration of 8.85×10^{13} spheres/cm^3, a measured surface charge of 2370 per sphere, a sphere radius of 83 nm and an impurity concentration (n_i) of 1.018×10^{17} ions/cm^3 ($=0.169$ mM; is assumed to be equal to n_pZ). Curve A shows that only compression occurs on heating. Curve B was calculated for the same parameters as that for curve A except that a renormalized surface charge of 1150 was used for curve B. Curve B indicates that the heated region contracts for low values of ΔT; s/d becomes increasingly more negative up to $\Delta T\approx5$ K after which it increases monotonically. The value of s/d crosses zero at $\Delta T\approx10$ K. This curve indicates that upon heating the crystal initially expands. The expansion is maximum when the central temperature is elevated by ca. 5 K. For higher ΔT values, the crystal only contracts. The inset of Fig. 4 shows the curve in the low ΔT region on an expanded scale for clarity. It is important to note that the crystal expands on heating even when the Coulomb pair potential decreases. This occurs because the positive temperature dependence of κ dominates the negative temperature dependence of U [Eq. (8)] for small values of ΔT (ca. 10 K); the temperature dependence of U dominates at larger values of ΔT.

The temperature at which expansion changes to contraction $(\Delta T)_r$ was calculated for various surface charge values and is shown in Fig. 5. From this figure it is clear that for charges $(Z)>1340$, no initial expansion is predicted while for $Z<1340$ an initial expansion occurs and the $(\Delta T)_r$ increases with decreasing charge. The inset in Fig. 5 is a plot of the maximum expansion as a function of surface charge. This plot shows that the maximum expansion decreases with increasing charge and there is no expansion for $Z>1340$. Obviously, if the extent of the linear deformation or if the temperature rise in the heated region is measured, Fig. 5 can be used to calculate the renormalized charge.

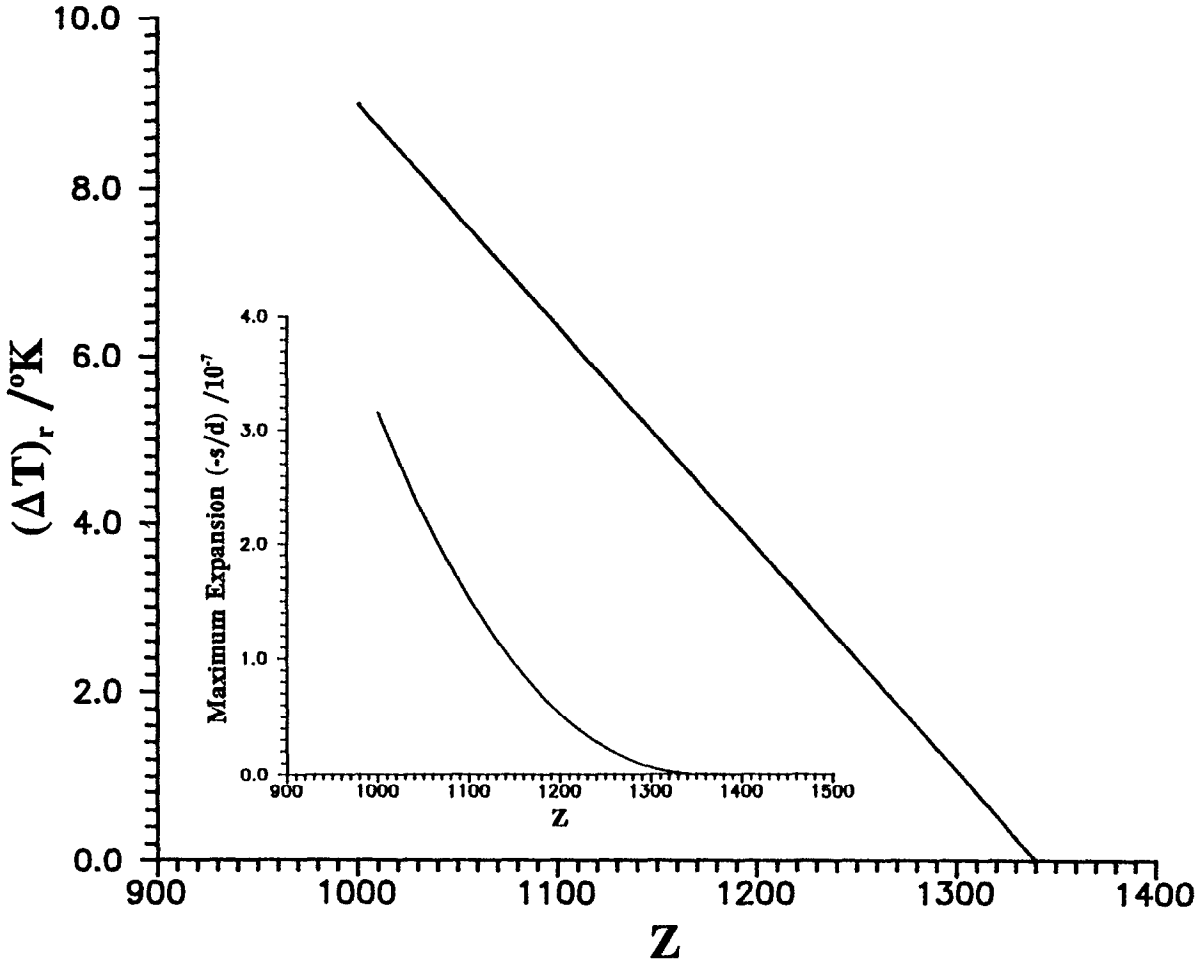

FIG. 5. Plot of the temperature rise required for the crystal strain to change from expansion to compression as a function of the sphere surface charge. The inset shows the maximum expansion possible for various values of surface charge.

For the colloid used here we observe an expansion during the first 100 ms after which compression sets in. This indicates that the effective charge on the particles is less than 1340. Because the value of charge on the particle was measured to be 2370 it is clear that charge renormalization is required to use the screened Coulomb pair potential function. Using the renormalization procedure of Alexander *et al.*,[9] we calculate the renormalized charge to be 1150 and we use this value in all of our subsequent calculations. For this value of renormalized charge, $(\Delta T)_r$ turns out to be 5 K and the calculated maximum expansion (s/d) from Fig. 5 is -9.6×10^{-8}.

We can determine the maximum compression of the crystal and the corresponding ΔT_{max} for various pump powers and pump durations using the determined values of the initial expansion of the crystal. The observed maximum transmittance, I_{T1}, in Fig. 1 occurs when the crystal expansion is a maximum $(s/d = -9.6\times10^{-8})$. Similarly, the observed minimum transmittance, I_{T2}, occurs when the crystal is maximally compressed. Hence, the maximum compression can be related to the transmittance by

$$\left(\frac{s}{d}\right)_{max} = -9.6\times10^{-8}\frac{(I_{T0}-I_{T2})}{(I_{T0}-I_{T1})}, \qquad (12)$$

where I_{T0} is the observed transmittance at $t=0$. The total net crystal strain is extremely small (Fig. 4) and occurs on an essentially linear portion of the diffraction peak as evident from Figure 9(c) of Rundquist *et al.*[14] Given this value of $(s/d)_{max}$ we can use curve B of Fig. 4 to determine ΔT_{max}. I_{T1}/I_{T0} is observed to be the same for all pump powers and pump durations because the crystal maximally expands at $\Delta T\sim5$ K. I_{T2}/I_{T0} depends on the pump power and pump duration, because the maximum ΔT in the crystal increases with increasing pump power and duration.

Figure 6 shows the calculated value of ΔT_{max} as a function of pump power for pump durations of 1 s and 0.5 s. The value of ΔT_{max} maximizes at about 30 K for the 0.5 s pulse. This saturation occurs because the thermal loss from the hot region to the surrounding cold region increases with temperature. The temperature increase of the hot region will also be a nonlinear function of the pump duration (for a given pump power). This is clearly illustrated in Fig. 6 where the difference in the slopes of the 1 and 0.5 s data is less than the expected factor of 2.

The ΔT_{max} which occurs for a 1 s pump duration with 50 mW of laser power can be independently estimated to check the value derived from the model. The decadic absorptivity of the dyed and undyed colloidal crystals of thickness 0.05 cm ($= b$) was measured to be 0.187 and 0.720, respectively. Assuming that the absorptivity of the undyed crystal comes from scattering from defects and phonons, the increased absorptivity of the dyed crystal (0.533) comes from the dye molecular absorption. The absorbed power, P, is calculated to be 27 mW. The maximum temperature rise in the crystal due to this absorption occurs at the center of the beam and can be determined from Eq. (16) of Dovichi:[28]

$$\Delta T_{max} = \frac{P}{2\pi kb}\int_0^1 \frac{dt'}{(\tau_T + 2t')}, \qquad (13)$$

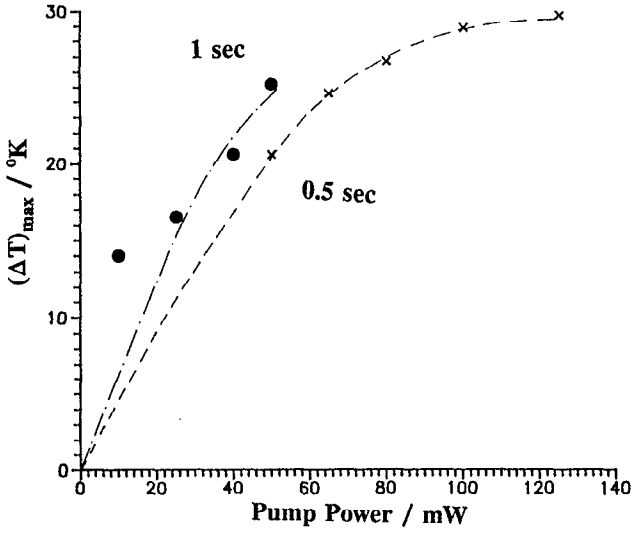

FIG. 6. Plot of the maximum temperature rise in the crystal as a function of the power of the pump laser beam. Pump duration of 0.5 s (×) or 1.0 s (●).

where k is the thermal conductivity of water and τ_T is the thermal diffusivity of water. Equation (13) gives a value of 33.7 K for ΔT_{max} whereas the present model gives 25.7 as seen from Fig. 6. Equation (13) overestimates ΔT_{max} because it ignores heat loss through the walls of the container where the colloid contacts the quartz.

The saturation of ΔT_{max} is also evident in the Fig. 1 data. The rate of decrease in the transmittance with time slows during the 1 s interval of crystal contraction which occurs while the pump beam is on. This decrease is most clearly evident for higher pump powers. During compression, ΔT and s increase. If ΔT increases linearly with time, the rate of decrease of transmittance will be constant only if s linearly follows ΔT. If s lags behind ΔT because of the low collective diffusion rate, the rate of decrease of transmittance will initially have a smaller slope than ΔT, but this slope will increase with time because the driving force for compression increases with time. The experimentally observed slowing rate of transmittance decrease indicates that the rate of increase in ΔT decreases with time.

For high pump powers (>25 mW) the crystal continues to compress even after the pump is turned off. This behavior is not seen for low pump powers. For high pump powers, the rate of increase of ΔT is high and the response of the particles is too slow to follow the changing ΔT; s lags behind. When the pump is turned off, the driving force for compression is still large and the particles continue to compress. For low pump powers the rate of increase of ΔT is sufficiently small that the change in s does not significantly lag behind the change in temperature.

The linear deformation model also accounts for the relaxation behavior. When the pump beam is turned off the compressed colloid must eventually expand. The initial driving force for expansion is zero, but δT and s are positive and differ from zero. The rapid thermal equilibration of the hot region in ca. 18 ms (the thermal equilibration time) causes

ΔT and δT to decrease to $\Delta T'$ and $\delta T'$. However, s cannot change significantly within this 18 ms time period because of the small collective particle diffusion coefficient.

The strain driving force (ΔF) which is zero at the transmission minima (Fig. 1) when the compressed colloid is about to expand, becomes increasingly positive with thermal equilibration. This increasing force causes the crystal to rapidly expand. As the value of s decreases ΔF becomes small, and the rate of particle motion can begin to follow the cooling rate. Hence, the relaxation curve shown in Fig. 1 will show two different rates which are evident at different time periods. These are illustrated in Fig. 1 by two straight lines, one with a large slope (immediately after the pump is turned off) and another with a much smaller slope, at longer times. In the longer time region ΔF is very small and because s follows $\Delta T'$, $\partial(\Delta F)/\partial t \simeq 0$. Assuming that only s and $\Delta T'$ depend on time and using Eq. (10), we get

$$\frac{\partial \Delta F}{\partial t} = 0 = \frac{\partial \delta T'}{\partial t}\left[\left(\kappa + \frac{1}{d}\right)\frac{\partial U}{\partial T} + U\frac{\partial \kappa}{\partial T}\right] + \frac{\partial s}{\partial t} U\left(\kappa^2 + \frac{2\kappa}{d} + \frac{2}{d^2}\right). \quad (14)$$

We can determine $\partial s/\partial t$ by using Eq. (12) and the Fig. 1 rate of increase of transmittance in step 2 of the relaxation process. The rate of decrease of the temperature, $\partial \delta T'/\partial t$ can be calculated using Eqs. (14) and (10). Figure 7 shows the calculated rate of cooling for the colloidal crystal heated to different values of ΔT. The rate of cooling nonlinearly increases with ΔT. This cooling rate differs from that for the illuminated region which we calculated earlier to be $\tau_T = 18$ ms. τ_T monitors the decay of the thermal gradient over the hot region, whereas the cooling here monitors the thermal relaxation over the entire crystal.

There are two thermal relaxation time processes involved. The fast 18 ms process involves relaxation of the thermal gradient within the probed portion of the sample; while the slower process (ca. 5 s) involves relaxation of the thermal gradient over the entire sample.

The two different thermal relaxation times derive from two different distance scales in the crystal. The 18 ms thermal relaxation time is associated with the thermal relaxation of the Gaussian-like thermal temperature distribution (which we approximate as a triangular distribution) within the probed region. This relaxes over the 200 μm beam width in the sample. This represents an experimentally defined relaxation time. In contrast, the ca. 5 s relaxation is defined by the macroscopic thermal properties of the colloidal crystal.

The decrease in ΔT during the 18 ms of thermal equilibration, ΔT_{th} (just after turning off the pump) can be obtained by extrapolating step 2 of the relaxation process of Fig. 1 back to $t = 1$ s. Let the extrapolated value of the transmittance at $t = 1$ s in the extrapolated line be I_{th}. The corresponding value of s/d and $\Delta T'$ can be obtained from Eqs. (12), (9), and (10). Hence, $\Delta T_{\text{th}} = \Delta T - \Delta T'$ can be calculated. Figure 8 shows ΔT_{th} for various ΔT. It is observed that ΔT_{th} increases almost linearly with ΔT. For small pump powers, ΔT_{th} is insignificant and the relaxation curve is a single straight line from the time the pump is turned off.

In the above discussion we have neglected any contribution to the lattice constant change which results from radiation pressure, photophoresis and thermophoresis.[32–36] We clearly can neglect the radiation pressure since the colloidal crystal of nonabsorbing spheres show no lattice changes. Further, we calculate that the magnitudes of radiation pressure, photophoresis, and thermophoresis are ca. 4 orders of magnitude less than the temperature dependent Coulombic interaction for the incident intensities we examine (< 200 W/cm^2).

CONCLUSION

We have developed a linear deformation model to explain photothermal phenomena in colloidal crystals, using

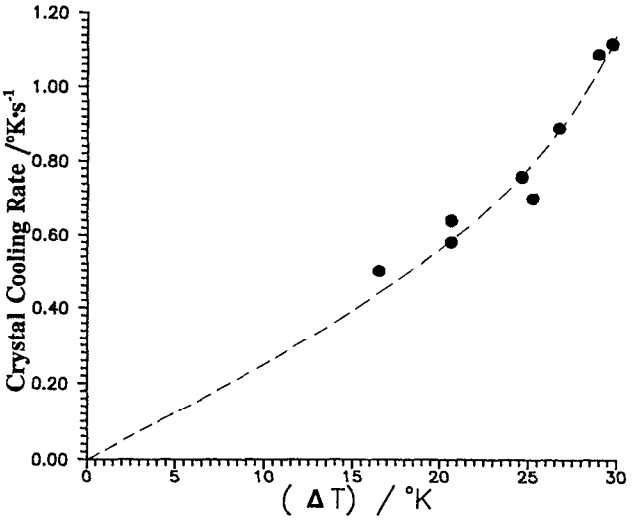

FIG. 7. Plot of the rate of cooling of the colloidal crystal as a function of the temperature rise in the crystal.

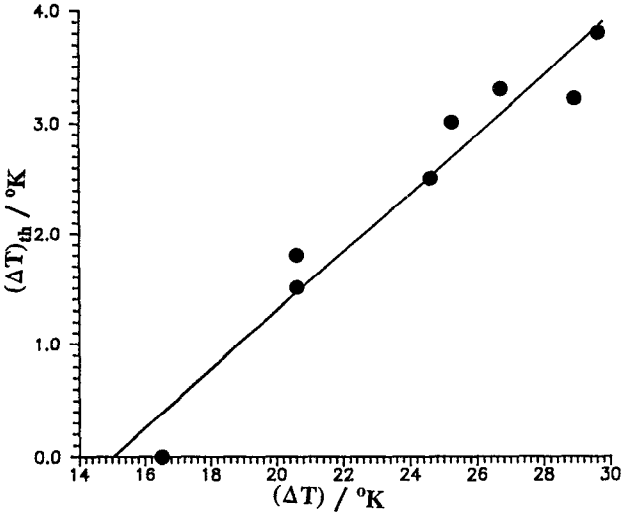

FIG. 8. Plot of the initial drop in temperature due to the thermal equilibration (after the pump is turned off) as a function of the temperature rise in the crystal.

the screened Coulomb pair potential. Using this model we can estimate the temperature increase in an absorbing colloidal crystal upon high intensity laser radiation. The photothermal response of these crystals can be used to examine the interparticle potential function. This study clearly indicates that the potential function only correctly predicts the interparticle potential if the colloid charge is renormalized. We demonstrate here a new photothermal technique which allows us to monitor the interparticle potential function and determine the required charge renormalization. Our studies also examine the colloidal crystal thermal relaxation rates.

ACKNOWLEDGMENT

We gratefully acknowledge funding for this work from a Ben Franklin Foundation grant from the Western Pennsylvania Advanced Technology Center.

[1] D. Thirumalai, J. Phys. Chem. **93**, 5637 (1989).
[2] R. Kesavamoorthy, A. K. Sood, B. V. R. Tata, and A. K. Arora, J. Phys. C **21**, 4737 (1988).
[3] M. O. Robbins, K. Kremer, and G. S. Grest, J. Chem. Phys. **88**, 3286 (1988).
[4] Y. Monovoukas and A. P. Gast, J. Colloid Interface Sci. **128**, 533 (1989).
[5] N. A. Clark and S. Safron, *Physics of Complex and Supermolecular Fluids* (Exxon Monographs) (Wiley–Interscience, New York, 1987).
[6] W. B. Russel, D. A. Saville, and W. R. Schowalter, *Colloidal Dispersions* (Cambridge University Press, New York, 1989).
[7] E. J. W. Vervey and J. Th. G. Overbeek, *Theory of the Stability of Lyophobic Colloids* (Elsevier, Amsterdam, 1948).
[8] B. V. Derjaguin and L. Landau, Acta Physicochim. URSS **14**, 633 (1941).
[9] S. Alexander, P. M. Chaikin, P. Grant, G. J. Morales, P. Pincus, and D. Hone, J. Chem. Phys. **80**, 5776 (1984).
[10] P. A. Hiltner and I. M. Krieger, J. Chem. Phys. **73**, 2386 (1969).
[11] S. A. Asher, P. L. Flaugh, and G. Washinger, Spectroscopy **1**, 26 (1986).
[12] P. L. Flaugh, S. E. O'Donnell, and S. A. Asher, Appl. Spectrosc. **38**, 847 (1984).
[13] S. A. Asher, U. S. Patents No. 4,627,689 and 4,632,517.
[14] P. A. Rundquist, P. Photinos, S. Jagannathan, and S. A. Asher, J. Chem. Phys. **91**, 4932 (1989).
[15] R. J. Spry and D. J. Kosan, Appl. Spectrosc. **40**, 782 (1986).
[16] B. J. Ackerson, in *Physics of Complex and Supermolecular Fluids*, edited by N. A. Clark and S. Safran (Exxon Monographs) (Wiley–Interscience, New York, 1987), p. 553.
[17] R. Kesavamoorthy and A. K. Arora, J. Phys. A **18**, 3389 (1985).
[18] R. J. Carlson and S. A. Asher, Appl. Spectrosc. **38**, 297 (1984).
[19] R. S. Crandall and R. Williams, Science **198**, 293 (1977).
[20] F. Richetti, J. Prost, and N. A. Clark, in *Physics of Complex and Supermolecular Fluids*, edited by N. A. Clark and S. Safran (Exxon Monographs) (Wiley–Interscience, New York, 1987), p. 387.
[21] T. Okubo, J. Chem. Soc. Faraday Trans I **84**, 1949 (1988).
[22] R. Williams, R. S. Crandall, and P. J. Wojtowicz, Phys. Rev. Lett. **37**, 348 (1976).
[23] J. G. Daly and R. Hastings, J. Phys. Chem. **85**, 294 (1981).
[24] T. Okubo, J. Chem. Soc. Faraday Trans I **82**, 3185 (1986).
[25] R. Kesavamoorthy, J. Phys. Condens. Matter **2**, 4273 (1990).
[26] S. Chandrasekhar, Rev. Mod. Phys. **15**, 1 (1943).
[27] Paul A. Rundquist, S. Jagannathan, R. Kesavamoorthy, Charles Brnardic, S. Xu, and Sanford A. Asher, J. Chem. Phys. **94**, 711 (1991).
[28] N. Dovichi, Crit. Rev. Anal. Chem. **17**, 357 (1987).
[29] F. Grüner and W. P. Lehmann, J. Phys. A **15**, 2847 (1982).
[30] P. N. Pusey and R. J. A. Tough, *Particle Interactions. In Dynamic Light Scattering: Application of Photon Correlation Spectroscopy*, edited by R. Pecora (Plenum, New York, 1985), pp. 85–179.
[31] R. Kesavamoorthy and A. Arora, J. Phys. C **19**, 2833 (1986).
[32] A. Chowdhury, B. J. Ackerson, and N. A. Clark, Phys. Rev. Lett. **55**, 833 (1985).
[33] A. Ashkin, Phys. Rev. Lett. **24**, 156 (1970).
[34] M. Kerker, Am. Sci. **62**, 92 (1974).
[35] O. Preining, in *Aerosol Science*, edited by C. N. Davies (Academic, New York, 1966).
[36] L. Waldmann and K. H. Schmitt, in *Aerosol Science*, edited by C. N. Davies (Academic, New York, 1966).